Key Points:

- There is a 95% chance that the time-averaged 2015–2100 volcanic SO_2 flux from explosive eruptions exceeds the time-averaged 1850–2014 flux
- Standard climate projections very likely underestimate the 2015–2100 stratospheric aerosol optical depth and volcanic climate effects
- Small-magnitude eruptions (<3 Tg SO_2) contribute 30%–50% of the volcanic climate effects in a median future eruption scenario

Author Contributions:

Conceptualization: Man Mei Chim, Thomas J. Aubry, Anja Schmidt
Data curation: Man Mei Chim, Nathan Luke Abraham, Lauren Marshall
Formal analysis: Man Mei Chim, Lauren Marshall
Funding acquisition: Man Mei Chim, Thomas J. Aubry, Jane Mulcahy, Jeremy Walton, Anja Schmidt
Investigation: Man Mei Chim
Methodology: Man Mei Chim, Thomas J. Aubry, Nathan Luke Abraham, Lauren Marshall, Anja Schmidt

Climate Projections Very Likely Underestimate Future Volcanic Forcing and Its Climatic Effects

Man Mei Chim[1] [ID], **Thomas J. Aubry[2]** [ID], **Nathan Luke Abraham[1,3]** [ID], **Lauren Marshall[4]**, **Jane Mulcahy[5]** [ID], **Jeremy Walton[5]** [ID], and **Anja Schmidt[1,6,7]**

[1]Yusuf Hamied Department of Chemistry, Centre for Atmospheric Science, University of Cambridge, Cambridge, UK, [2]Department of Earth and Environmental Sciences, University of Exeter, Penryn, UK, [3]National Centre for Atmospheric Science, Cambridge, UK, [4]Department of Earth Sciences, Durham University, Durham, UK, [5]Met Office, Exeter, UK, [6]German Aerospace Center (DLR), Institute of Atmospheric Physics (IPA), Oberpfaffenhofen, Germany, [7]Meteorological Institute, Ludwig-Maximilians University Munich, Munich, Germany

Abstract Standard climate projections represent future volcanic eruptions by a constant forcing inferred from 1850 to 2014 volcanic forcing. Using the latest ice-core and satellite records to design stochastic eruption scenarios, we show that there is a 95% probability that explosive eruptions could emit more sulfur dioxide (SO_2) into the stratosphere over 2015–2100 than current standard climate projections (i.e., ScenarioMIP). Our simulations using the UK Earth System Model with interactive stratospheric aerosols show that for a median future eruption scenario, the 2015–2100 average global-mean stratospheric aerosol optical depth (SAOD) is double that used in ScenarioMIP, with small-magnitude eruptions (<3 Tg of SO_2) contributing 50% to SAOD perturbations. We show that volcanic effects on large-scale climate indicators, including global surface temperature, sea level and sea ice extent, are underestimated in ScenarioMIP because current climate projections do not fully account for the recurrent frequency of volcanic eruptions of different magnitudes.

Plain Language Summary Climate projections are the simulations of Earth's climate in the future using complex climate models. Standard climate projections, as in Intergovernmental Panel on Climate Change Sixth Assessment Report, assume that explosive volcanic activity over 2015–2100 are of the same level as the 1850–2014 period. Using the latest ice-core and satellite records, we find that explosive eruptions could emit more sulfur dioxide into the upper atmosphere for the period of 2015–2100 than standard climate projections. Our climate model simulations show that the impacts of volcanic eruptions on climate, including global surface temperature, sea level and sea ice extent, are underestimated because current climate projections do not fully account for the recurrent frequency of volcanic eruptions. We also find that small-magnitude eruptions occur frequently and can contribute a significant effect on future climate.

1. Introduction

Large explosive volcanic eruptions can inject sulfur dioxide (SO_2) forming volcanic sulfate aerosols in the stratosphere that scatter incoming solar radiation, resulting in negative radiative forcing and global surface cooling for 1–3 years (McCormick et al., 1995). Stratospheric volcanic sulfate aerosols also heat the stratosphere by absorbing infrared and near-infrared radiation, which can further induce complex climate responses on seasonal to multi-decadal timescales (see Marshall et al., 2022 for a review).

As we cannot predict future volcanic eruptions, a constant volcanic forcing is commonly used in climate projections, for example, as done in Phase 6 of the Coupled Model Intercomparison Project (CMIP6; Eyring et al., 2016), which informs the Intergovernmental Panel on Climate Change (IPCC) Sixth Assessment Report. In the CMIP6 Scenario MIP (ScenarioMIP; O'Neill et al., 2016), the constant volcanic forcing is inferred from the time average of the reconstructed 1850–2014 volcanic forcing. This approach does not account for how the sporadic occurrence of volcanic eruptions may affect the climate as opposed to a time-averaged forcing. In addition, volcanic injections into the stratosphere during the Holocene (past 11,500 years; Sigl et al., 2022) can vary by as much as a factor of 25 on centennial timescales. The corresponding uncertainty on future volcanic forcing is currently unaccounted for in most climate projections. A handful of studies have attempted to quantify the role of volcanic forcing uncertainty in climate projections (Ammann & Naveau, 2010; Bethke et al., 2017; Dogar et al., 2020). Bethke et al. (2017) estimated the volcanic forcing of 60 different future eruption scenarios from 2015 to 2100 by resampling ice-core sulfate deposition records going back 2,500 years (Sigl et al., 2015).

Resources: Thomas J. Aubry, Nathan Luke Abraham, Jane Mulcahy, Jeremy Walton, Anja Schmidt
Supervision: Thomas J. Aubry, Nathan Luke Abraham, Anja Schmidt
Visualization: Man Mei Chim
Writing – original draft: Man Mei Chim
Writing – review & editing: Man Mei Chim, Thomas J. Aubry, Nathan Luke Abraham, Lauren Marshall, Jane Mulcahy, Jeremy Walton, Anja Schmidt

Up-to-date ice-core and satellite volcanic sulfur emission datasets enable us to account for the occurrence of (a) eruptions larger in magnitude than those that occurred between 1850 and 2014, which injected as much as 300 Tg of SO_2 into the atmosphere, and (b) small-magnitude eruptions below the detection threshold of ice-core datasets (Figure 1a), which can contribute a significant fraction to stratospheric aerosol optical depth (SAOD) (Santer et al., 2014; Schmidt et al., 2018).

In addition, whether they apply a constant volcanic forcing (e.g., CMIP6 ScenarioMIP) or use stochastic eruption scenarios (Bethke et al., 2017), existing climate projections use prescribed volcanic aerosol optical properties derived from simplified volcanic aerosol models. Climate models with interactive stratospheric aerosols (Timmreck et al., 2018) showed a better agreement between the simulated surface temperature responses and tree-ring surface temperature reconstructions for the 1257 Mount Samalas and 1815 Mount Tambora eruptions (Stoffel et al., 2015) and the 1783–1784 Laki eruption (Pausata et al., 2015; Zambri et al., 2019). Furthermore, the prescribed aerosol approach cannot account for the impacts of global warming on the life cycle of volcanic sulfate aerosols (Aubry et al., 2021), including the impact of changing atmospheric stratification on volcanic plume height (Aubry et al., 2019). Such climate-volcano feedbacks might amplify the peak global-mean radiative forcing associated with large-magnitude tropical eruptions by 30% (Aubry et al., 2021).

Our study aims to improve our understanding of future volcanic impacts on climate. To this end, we perform model simulations from 2015 to 2100 with two innovations: (a) a stochastic resampling approach using the latest ice-core and satellite datasets to generate improved future volcanic eruption scenarios; and (b) a plume-aerosol-chemistry-climate modeling framework (named UKESM-VPLUME), which combines a volcanic plume model and an Earth System Model with interactive stratospheric aerosols to simulate volcanic climate effects while accounting for climatic controls on plume-rise height.

2. Methodology

2.1. Stochastic Future Eruption Scenarios

We generate 1,000 stochastic future eruption scenarios for 2015–2100 by resampling SO_2 mass from volcanic emission inventories from a bipolar ice-core array covering the past 11,500 years (Holvol; Sigl et al., 2022) and a multi-satellite record from 1979 to 2021 (S. Carn, 2022; S. A. Carn et al., 2016) (Figure 1a and Figure S1 in Supporting Information S1). Before resampling, we filter out: (a) effusive eruptions; (b) in the satellite record, eruptions with eruptive plume heights more than 3 km below the thermal tropopause (obtained from NCEP/NCAR Reanalysis 1; Kalnay et al., 1996); we assume that aerosol lofting could result in stratospheric injections for tropospheric plumes less than 3 km below the tropopause. By examining the eruption frequency-magnitude (i.e., in this study, SO_2 mass) distribution of both ice-core and satellite records (Figure 1a), we identify 3 Tg of SO_2 as a threshold: (a) below which ice-core records underestimate eruption frequency due to under-recording; and (b) above which the short duration of the satellite record precludes it from capturing the true frequency of eruptions with higher magnitude. Accordingly, we use a 3 Tg of SO_2 threshold to define "small-magnitude" and "large-magnitude" eruptions. We resample small-magnitude eruptions from the satellite record only, and large-magnitude ones from the combined ice-core and satellite record. Details of the resampling procedures are discussed in Supporting Information S1.

2.2. UKESM-VPLUME

Atmospheric stratification, wind and humidity affect volcanic plume dynamics and SO_2 injection height (e.g., Mastin, 2014), but SO_2 height is commonly prescribed in modeling studies of volcanic forcing (e.g., Timmreck et al., 2018). To account for meteorological controls on plume dynamics, we have developed UKESM-VPLUME, which couples the UK Earth System Model (UKESM; Mulcahy et al., 2023) with Plumeria (1-D eruptive plume model; Mastin, 2007, 2014) (details in Supporting Information S1). We use version 1.1 of UKESM with fully-coupled atmosphere-land-ocean and interactive stratospheric aerosols. In brief, for each time step of the UKESM atmospheric model during an eruption, UKESM-VPLUME interactively passes the atmospheric conditions simulated at the eruption location to Plumeria. Plumeria then computes the neutral buoyancy height of the volcanic plume based on atmospheric conditions and the mass eruption rate generated for each eruption in the stochastic scenarios. Volcanic SO_2 is injected into UKESM at the neutral buoyancy height calculated in Plumeria using a Gaussian profile with a width of 10% of the plume height (consistent with large-eddy
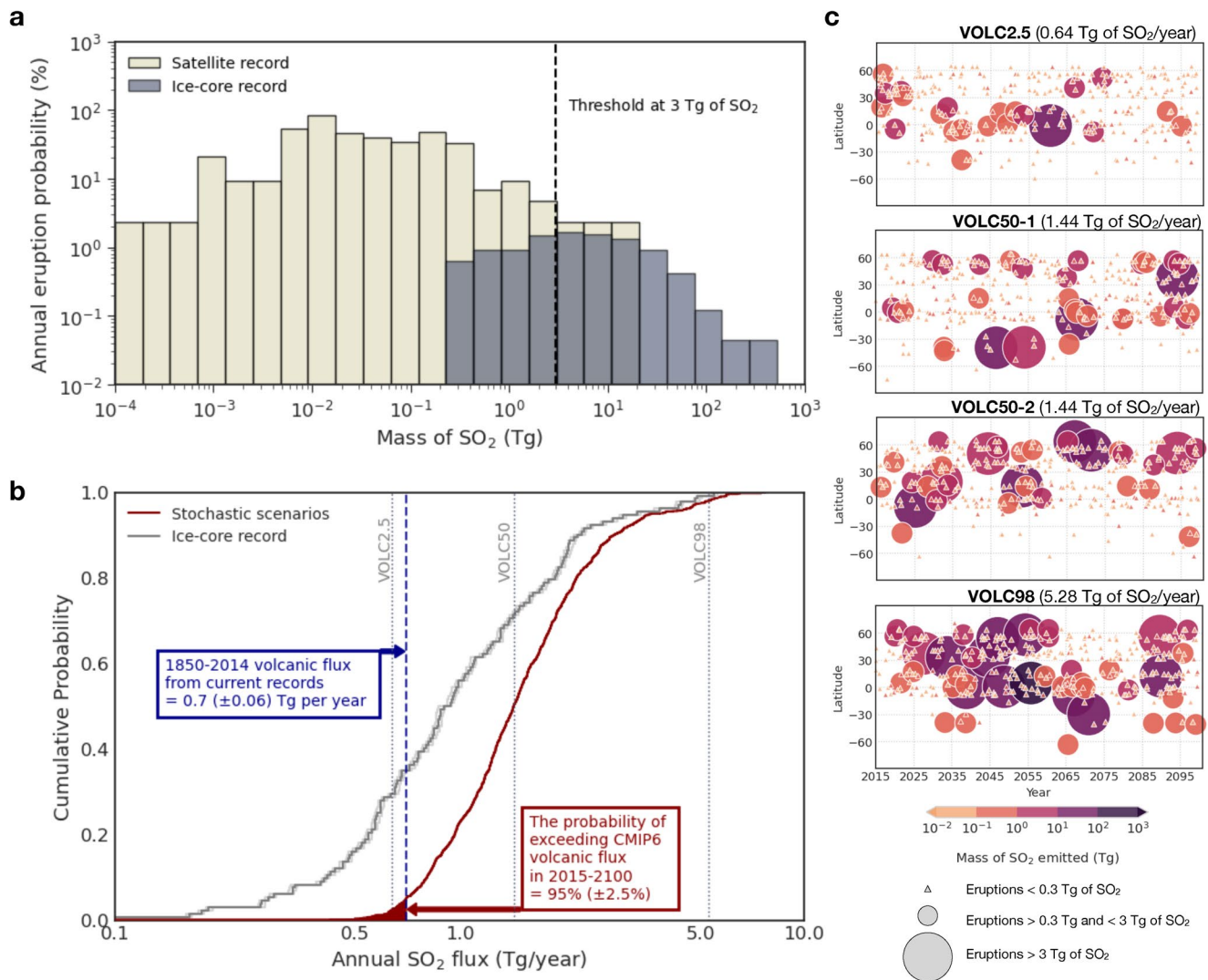
Figure 1. (a) Annual eruption probability based on ice-core (Sigl et al., 2022) and satellite (S. Carn, 2022) datasets. (b) Empirical cumulative probability density function of the SO_2 mass distribution of the 1,000-member stochastic scenarios and the Holvol ice-core dataset (95% bootstrap confidence bounds in light gray). We estimate the probability of exceeding CMIP6 volcanic flux using the 1850–2014 flux from current volcanic emission inventories (S. Carn, 2022; Neely & Schmidt, 2016; Sigl et al., 2022). (c) Eruption time series of VOLC2.5, VOLC50-1, VOLC50-2, and VOLC98 with annual volcanic SO_2 flux of each scenario in brackets.

simulations of volcanic plumes, Aubry et al., 2019). This approach ensures that plume heights of volcanic eruptions are consistent with the meteorological conditions simulated by UKESM.

2.3. Experimental Design

We perform simulations using the UKESM-VPLUME framework for four stochastic future eruption scenarios at the 2.5th, 50.0th, 50.5th and 98.0th percentiles (termed VOLC2.5, VOLC50-1, VOLC50-2, VOLC98) of the distribution of the 2015–2100 average SO_2 flux across the 1,000 future eruption scenarios (Figure 1b). We choose scenarios close (within 0.5 percentile) to the 2.5th, 50th and 97.5th to sample the median and 95% confidence interval of the future volcanic stratospheric SO_2 injections. To test future climate trajectory sensitivity to the temporal and spatial distribution of eruptions, we run two scenarios near the 50th percentile. For instance, VOLC50-2 has more large-magnitude eruptions than VOLC50-1 in the early 21st century (Figure 1c). We also performed the VOLC50 runs with small-magnitude eruptions only (VOLC50-1S and VOLC50-2S) to isolate their contribution to the overall climate effects caused by eruptions of all magnitudes. We compare the results from
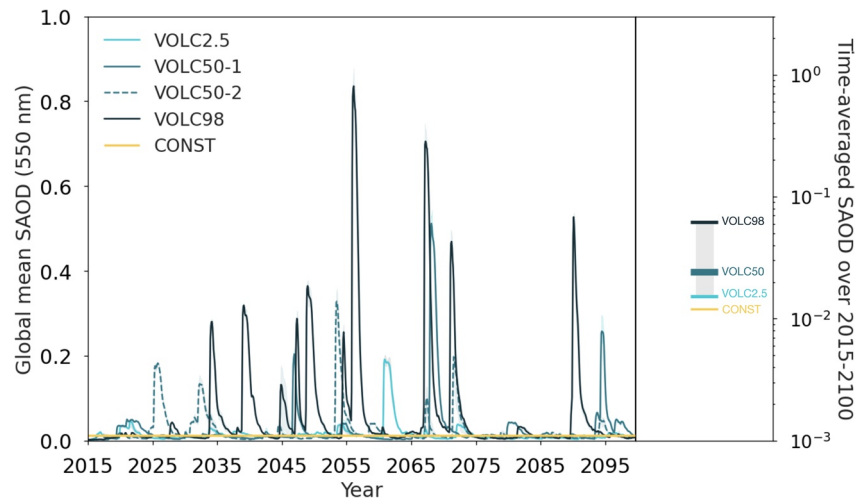
Figure 2. (Left) Global monthly-mean stratospheric aerosol optical depth (SAOD) at 550 nm. The lines show the ensemble mean and the shading shows the spread of the maximum and minimum ensemble members. (Right) The corresponding time-averaged SAOD over 2015–2100 (in log scale).

VOLC runs with runs without volcanic eruptions (NOVOLC) and with CMIP6 ScenarioMIP constant volcanic forcing (CONST). We perform all simulations from 2015 to 2100 under a high-end future shared socio–economic pathway (SSP) scenario (SSP3-7.0 in ScenarioMIP) running three ensemble members for each scenario.

3. Results

Figure 2 shows the global monthly-mean SAOD at 550 nm and the time-averaged values over 2015–2100. The time-averaged ensemble-mean SAOD ranges from 0.015 ± 0.0004 (VOLC2.5, one standard deviation uncertainty) to 0.062 ± 0.0018 (VOLC98), with an average value of 0.024 ± 0.0012 for the two median future eruption scenarios (VOLC50), while the SAOD in CONST, which followed the ScenarioMIP design, is 0.012 ± 0.0018. Small-magnitude eruptions contribute 0.010–0.013 ± 0.0002 to the time-averaged SAOD in the VOLC50 scenarios, that is, about 50% of the total SAOD. Comparing VOLC2.5 to CONST and assuming that the rank for the 2015–2100-year mean volcanic SO_2 flux and SAOD are the same, it is thus very likely (i.e., >90% probability following IPCC guidance note; Mastrandrea et al., 2010) that the actual global 2015–2100 mean SAOD will be higher than that prescribed in ScenarioMIP, with the median (VOLC50) SAOD value being double that used in ScenarioMIP. The result is consistent with Figure 1, given that the 1850–2014 time-averaged SO_2 flux used to define the ScenarioMIP volcanic forcing is close to the 2.5th percentile of the future volcanic SO_2 flux distribution. Beyond the time-averaged SAOD value, owing to the sporadic nature of volcanic eruptions, the global monthly-mean SAOD values in VOLC scenarios can be up to a factor of 60 greater than that in ScenarioMIP (Figure 2 and Figure S2 in Supporting Information S1).

Figure 3a shows the global annual-mean surface air temperature at 1.5 m (GMST) relative to the 1850–1900 period. Large-magnitude volcanic eruptions lead to a short-term drop in the annual-mean GMST for at least 1 year and up to 6–7 years for the largest eruptions. In the VOLC98 scenario where clusters of large-magnitude eruptions occur, they can induce multi-decadal global cooling. The 2015–2100 time-averaged GMST relative to detrended NOVOLC ensemble mean (Figure 3b) ranges between −0.16°C (VOLC2.5) and −0.56°C (VOLC98), with CONST lying outside this range at −0.12°C. Volcanic cooling for median eruption scenarios (VOLC50-1 and VOLC50-2) is 0.20–0.24°C, double that of CONST, and 0.09–0.10°C of cooling is attributable to small-magnitude eruptions (Table S1 in Supporting Information S1).

The IPCC defines global warming as an increase, relative to 1850–1900, in the global mean surface air and sea surface temperatures over a period of 30 years (IPCC, 2021). Using this definition, we examine the year of crossing of 1.5, 2, and 3°C warming thresholds for VOLC and CONST runs (Figure 3c). Volcanic eruptions delay the time of crossing 1.5°C by about 1.6–3.2 years when compared to NOVOLC (Table S2 in Supporting Information S1), consistent with Bethke et al. (2017). Compared to CONST, times of temperature threshold crossings are
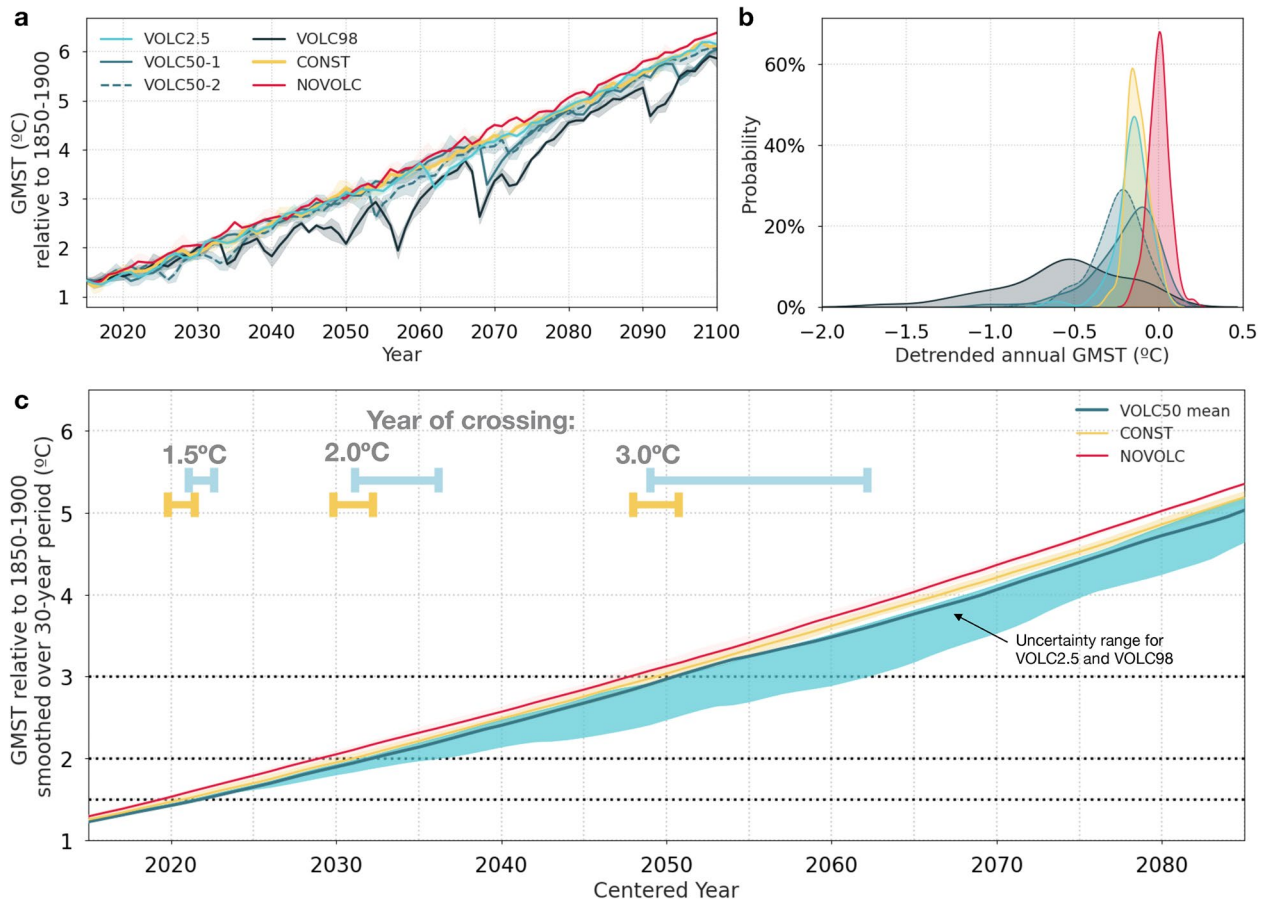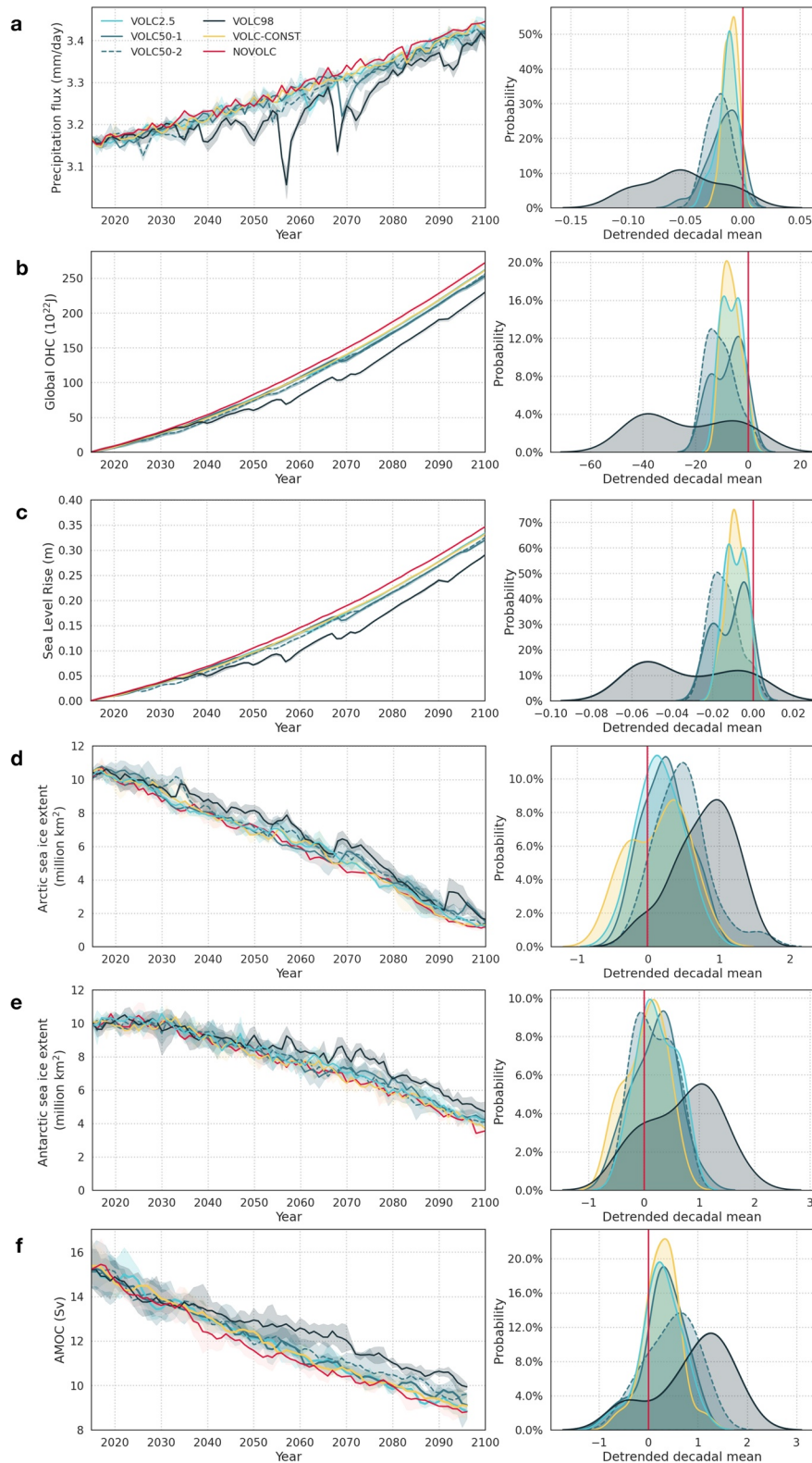
Figure 3. (a) Annual-mean GMST relative to 1850–1900. The lines show the ensemble mean and the shading shows the spread of the maximum and minimum ensemble members. (b) Probability density function of the annual-mean GMST relative to detrended NOVOLC ensemble mean (see Supporting Information S1). (c) 30-year moving mean GMST with years of crossing 1.5, 2, and 3°C for VOLC and CONST runs.

significantly delayed by 1.8–2.5 years in VOLC50-2, but unaffected in VOLC50-1. This highlights the sensitivity of the time of crossing to the temporal distribution of large-magnitude eruptions. The occurrence of volcanic clusters in VOLC98 causes an extended cooling period between 2034 and 2060 (Figure 3a) which delays the crossing of 2 and 3°C by 7 and 14 years, respectively.

In Figure 4, we examine volcanic effects on large-scale climate indicators other than GMST. The 2015–2100 time-averaged global annual-mean precipitation fluxes in all VOLC runs show a greater reduction than CONST, with a range between −0.014 mm/day (VOLC2.5) to −0.052 mm/day (VOLC98), and −0.010 mm/day for CONST (Figure 4a). In VOLC50 scenarios, the global annual-mean precipitation flux is reduced by 0.019 mm/day with small-magnitude eruptions alone contributing between 0.008 and 0.009 mm/day, comparable to the effects of the volcanic forcing implemented in ScenarioMIP. It is thus very likely that the reduction of global mean precipitation due to volcanic effects is underestimated in ScenarioMIP.

Volcanic-induced surface cooling penetrates into the deep ocean layer and decreases the global ocean heat content (Figure 4b and Figure S3 in Supporting Information S1), which in turn leads to less thermal expansion in seawater and a reduction in thermosteric sea level (Figure 4c). Volcanic forcing in VOLC50 reduces global ocean heat content and thermosteric sea level by 6%–7% compared to NOVOLC by 2100, whereby about half is attributed to small-magnitude eruptions (Figure S3 in Supporting Information S1). Although volcanic forcing can cause considerable impacts on large-scale ocean metrics, it does not offset the anthropogenic-induced ocean warming trends even for the upper-end volcanic emission scenario VOLC98 (Figures 4b, 4c, and 4f).

Depending on the eruption magnitude and location, the Arctic and Antarctic sea ice extents show an immediate increase for 1–2 years after large-magnitude eruptions (Figures 4d and 4e). The time-averaged global

Figure 4. (Left) Annual-mean time series of selected large-scale climate indicators. The line shows the ensemble mean and the shading shows the spread of the maximum and minimum ensemble members. (Right) The corresponding decadal-mean probability density function relative to the detrended NOVOLC ensemble mean, with red vertical line showing the mean of NOVOLC. (a) Global precipitation flux (mm/day), (b) global ocean heat content (10^{22} J), (c) global thermosteric sea level rise (m), (d and e) Arctic and Antarctic sea ice extent (million km^2), defined as the area with >15% sea ice, (f) 5-year moving mean Atlantic Meridional Overturning Circulation at 26°N (Sv).

sea ice extent in VOLC runs over 2015–2100 increases by 0.43 million km^2 (VOLC2.5) to 1.53 million km^2 (VOLC98) as compared to 0.20 million km^2 for CONST. Comparing VOLC2.5 to CONST suggests that for similar time-averaged SAOD, the use of a constant forcing instead of a stochastic eruption distribution halves the magnitude of the sea ice response.

The time-averaged Atlantic Meridional Overturning Circulation (AMOC) at 26°N over 2015–2100 is strengthened by between 0.26 Sv (VOLC2.5) and 0.93 Sv (VOLC98) as compared to NOVOLC, with all VOLC scenarios exhibiting an increased decadal mean AMOC strength (Figure 4f). Small-magnitude eruptions alone can increase the time-averaged AMOC strength by 0.36–0.38 Sv (VOLC50-1S and VOLC50-2S), which is greater than CONST at 0.28 Sv, and contribute to over 77% of the AMOC response in the median future scenarios (Table S1 in Supporting Information S1). One of the median future scenarios (VOLC50-1) has a weaker time-averaged AMOC response than the same run with small-magnitude eruptions only (VOLC50-1S) due to an extended period of weakened AMOC after the occurrence of large-magnitude eruptions with aerosols dispersed to the Southern Hemisphere (Figures S2 and S4 in Supporting Information S1). Our results suggest that AMOC may have different responses caused by differences in the asymmetries of the stratospheric aerosol burdens from large-magnitude eruptions, which warrants further investigation.

4. Discussion

Small-magnitude eruptions (<3 Tg of SO_2) contribute a considerable fraction (between 33% and 40%) of the total upper atmospheric volcanic SO_2 emissions in VOLC50, and in turn, are responsible for 30%–50% of the volcanic impact on selected large-scale climate indicators and over 77% of the AMOC response (Figure 5 and Table S1 in Supporting Information S1). For future eruption scenarios with fewer eruptions than VOLC50, the contribution from small-magnitude eruptions is expected to be even greater because the total mass injected by small-magnitude eruptions is relatively similar across all scenarios. Despite the importance of volcanic forcing from small-magnitude eruptions, they are mostly unaccounted for in historical simulations before satellite measurements are available. In the pre-satellite historical period (1850–1978), the Neely and Schmidt (2016) and Sigl et al. (2022) volcanic SO_2 inventories have an average flux of 0.21 and 0.26 Tg of SO_2 per year from small-magnitude eruptions, respectively. By comparison, the flux is 0.52 Tg of SO_2 per year over 1980–2020 (S. Carn, 2022; 0.63 Tg of SO_2 per year over 2001–2020 with better satellite measurements). This suggests a missing flux from small-magnitude eruptions of between 0.26 and 0.31 Tg of SO_2 per year over 1850–1978, which is the equivalent of injections from about 2 to 3 Mount Pinatubo 1991 eruptions.

Our stochastic scenarios imply that CMIP6 ScenarioMIP very likely (95 ± 2.5%) underestimates the 2015–2100 volcanic SO_2 flux from explosive eruptions and, in turn, forcing (Figure 1b). Figure 1b shows the cumulative probability against the annual SO_2 flux obtained by resampling ice-core record of volcanic SO_2 injection only (i.e., Holvol; Sigl et al., 2022) and both ice-core and satellite (S. Carn, 2022) records as in our stochastic scenarios. CMIP6 ScenarioMIP uses a constant volcanic forcing inferred from the 1850–2014 period during which the mean volcanic SO_2 flux recorded in emission inventories was 0.7 ± 0.06 Tg per year. However, we find a 95% confidence interval for the 2015–2100 mean volcanic SO_2 flux between 0.64 and 5.28 Tg per year in our eruption scenarios (Figure 1b). Our stochastic approach, which represents better the frequency-magnitude distribution of small-magnitude eruptions, results in a higher annual SO_2 flux than resampling from the ice-core record only (e.g., Bethke et al., 2017).

Our future volcanic eruption scenarios greatly enhance the variability of large-scale climate indicators as compared to the ScenarioMIP forcing (Figure 5). Future volcanic emissions in our scenarios cause a 3.5% (VOLC2.5) to 15.0% (VOLC98) decrease in the 2015–2100 time-averaged global net radiative forcing at the top-of-the-atmosphere relative to the anthropogenic contribution (Figure 5 and Figure S5 in Supporting Information S1). The time-averaged climate responses of our selected climate indicators scale with the magnitude of volcanic forcing except for the Antarctic sea ice extent and AMOC, which may depend on the latitudinal distribution of eruptions. We also find that the magnitude of volcanic effects on climate indicators are comparable between CONST and VOLC2.5, which is a scenario with only one Pinatubo-like eruption over 2015–2100. Our results suggest that due to the low volcanic forcing used in ScenarioMIP, it is very likely (97.5%) that ScenarioMIP underestimates the climate effects of the large-scale climate indicators examined in this study.

Our simulation results show that for the SSP3-7.0 scenario, volcanic forcing can offset 2.1%–18.2% of the anthropogenic effects to large-scale climate indicators depending on the future eruption scenarios (Figure 5). In a future
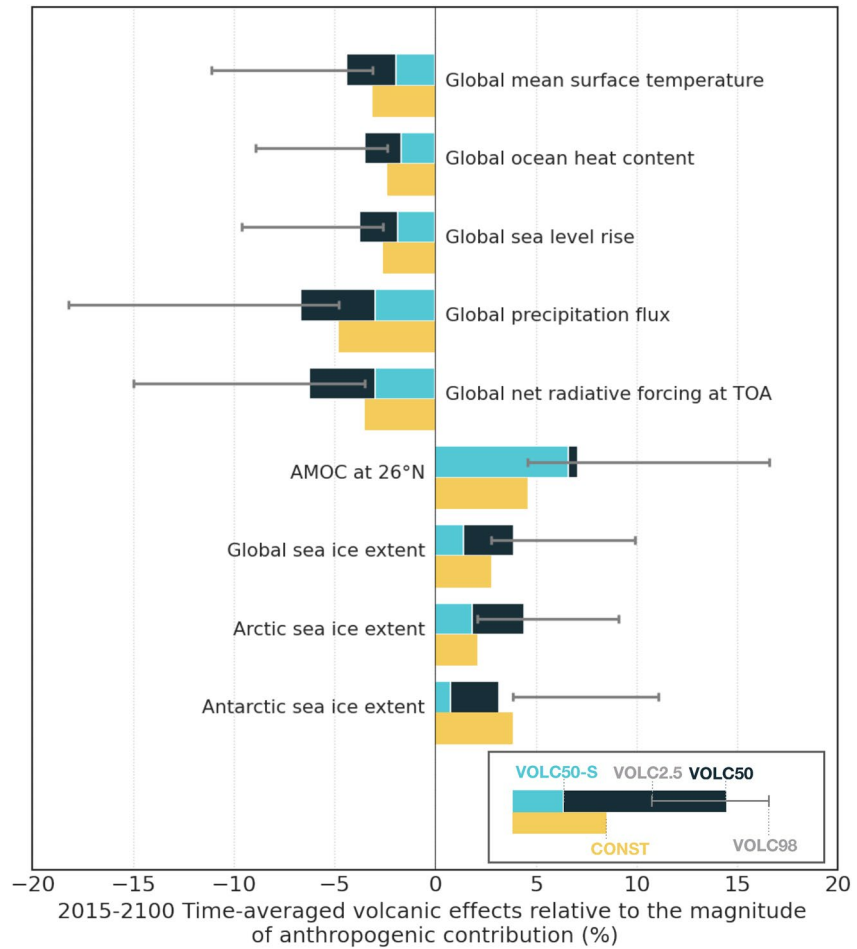
Figure 5. Bar chart showing the time-averaged volcanic effects on large-scale climate indicators relative to the magnitude of anthropogenic contribution over the period of 2015–2100, that is, $\frac{\overline{\text{VOLC}-\text{NOVOLC}}}{|\text{NOVOLC}_{2100}-\text{NOVOLC}_{2015}|}$. VOLC50-S refers to average effects of the two VOLC50 runs with small-magnitude eruptions.

scenario with low-end anthropogenic emission, we would expect the relative effect between future volcanism and anthropogenic forcing to be much greater. Our work highlights how the high level of uncertainty on volcanic forcing affects climate projections. For the same future eruption scenario, the volcanic effects on climate will also vary between SSP scenarios owing to climate-volcano feedbacks (e.g., Aubry et al., 2022; Fasullo et al., 2018; Hopcroft et al., 2018), which need to be quantified.

5. Conclusion

We performed climate model simulations from 2015 to 2100 with stochastic future eruption scenarios using UKESM-VPLUME (a plume-aerosol-chemistry-climate model framework that accounts for climate-volcano feedbacks) to examine how the uncertainties on volcanic forcing affect climate projections. Using the latest ice-core and satellite datasets, we show that the 2015–2100 volcanic SO_2 flux from explosive eruptions has a 95% probability to exceed the 1850–2014 flux, which was used to derive volcanic forcing in CMIP6 ScenarioMIP. Our simulations suggest that the time-averaged SAOD in a median future scenario is 0.024 (95% uncertainty: 0.015–0.062), which is double that in ScenarioMIP, and that ScenarioMIP very likely underestimates the future volcanic effects on climate. Our study emphasizes the importance of the climate effects of future volcanic eruptions relative to the anthropogenic contribution, which even for an upper end anthropogenic forcing scenario (SSP3-7.0) can range between 2.1% and 18.2% for large-scale climate indicators. We also highlight the climate-relevance of small-magnitude eruptions, which are responsible for 30%–50% of the volcanic

effects on selected climate indicators. Future CMIP experiment designs should update historical forcings for the pre-satellite historical period (1850–1978) to include volcanic sulfur emissions from small-magnitude eruptions in this period, and ideally use interactive stratospheric aerosols that can explicitly simulate climate-volcano feedbacks. Future climate projection studies should either use stochastic eruption scenarios generated using state-of-the-art volcanic emission inventories or time-averaged constant forcing derived from such scenarios that better represents long-term volcanic activity.

Conflict of Interest

The authors declare no conflicts of interest relevant to this study.

Data Availability Statement

The data presented in this study are available in the University of Cambridge data repository: https://doi.org/10.17863/CAM.94912. All data used for this study is with the license Creative Commons Attribution 4.0 International (CC-BY-4.0).

References

Ammann, C. M., & Naveau, P. (2010). A statistical volcanic forcing scenario generator for climate simulations. *Journal of Geophysical Research*, *115*(D5), D05107. https://doi.org/10.1029/2009JD012550

Aubry, T. J., Cerminara, M., & Jellinek, A. M. (2019). Impacts of climate change on volcanic stratospheric injections: Comparison of 1-D and 3-D plume model projections. *Geophysical Research Letters*, *46*(17–18), 10609–10618. https://doi.org/10.1029/2019GL083975

Aubry, T. J., Farquharson, J. I., Rowell, C. R., Watt, S. F., Pinel, V., Beckett, F., et al. (2022). Impact of climate change on volcanic processes: Current understanding and future challenges. *Bulletin of Volcanology*, *84*(6), 1–11. https://doi.org/10.1007/s00445-022-01562-8

Aubry, T. J., Staunton-Sykes, J., Marshall, L. R., Haywood, J., Abraham, N. L., & Schmidt, A. (2021). Climate change modulates the stratospheric volcanic sulfate aerosol lifecycle and radiative forcing from tropical eruptions. *Nature Communications*, *12*(1), 4708. https://doi.org/10.1038/s41467-021-24943-7

Bethke, I., Outten, S., Otterå, O. H., Hawkins, E., Wagner, S., Sigl, M., & Thorne, P. (2017). Potential volcanic impacts on future climate variability. *Nature Climate Change*, *7*(11), 799–805. https://doi.org/10.1038/nclimate3394

Carn, S. (2022). Multi-satellite volcanic sulfur dioxide L4 long-term global database V4 (MSVOLSO2L4 4) [Dataset]. Goddard Earth Science Data and Information Services Center (GES DISC). Retrieved from https://disc.gsfc.nasa.gov/datasets/MSVOLSO2L4_4/summary

Carn, S. A., Clarisse, L., & Prata, A. J. (2016). Multi-decadal satellite measurements of global volcanic degassing. *Journal of Volcanology and Geothermal Research*, *311*, 99–134. https://doi.org/10.1016/j.jvolgeores.2016.01.002

Dogar, M. M., Sato, T., & Liu, F. (2020). Ocean sensitivity to periodic and constant volcanism. *Scientific Reports*, *10*(1), 293. https://doi.org/10.1038/s41598-019-57027-0

Eyring, V., Bony, S., Meehl, G. A., Senior, C. A., Stevens, B., Stouffer, R. J., & Taylor, K. E. (2016). Overview of the Coupled Model Intercomparison Project Phase 6 (CMIP6) experimental design and organization. *Geoscientific Model Development*, *9*(5), 1937–1958. https://doi.org/10.5194/gmd-9-1937-2016

Fasullo, J. T., Tilmes, S., Richter, J. H., Kravitz, B., MacMartin, D. G., Mills, M. J., & Simpson, I. R. (2018). Persistent polar ocean warming in a strategically geoengineered climate. *Nature Geoscience*, *11*(12), 910–914. https://doi.org/10.1038/s41561-018-0249-7

Hopcroft, P. O., Kandlbauer, J., Valdes, P. J., & Sparks, R. S. J. (2018). Reduced cooling following future volcanic eruptions. *Climate Dynamics*, *51*(4), 1449–1463. https://doi.org/10.1007/s00382-017-3964-7

IPCC. (2021). In V. Masson-Delmotte, P. Zhai, A. Pirani, S. L. Connors, C. Péan, et al. (Eds.), *Climate change 2021: The physical science basis. Contribution of Working Group I to the sixth assessment report of the Intergovernmental Panel on Climate Change*. Cambridge University Press. (In press). https://doi.org/10.1017/9781009157896

Kalnay, E., Kanamitsu, M., Kistler, R., Collins, W., Deaven, D., Gandin, L., et al. (1996). The NCEP/NCAR 40-year reanalysis project. *Bulletin of the American Meteorological Society*, *77*(3), 437–472. https://doi.org/10.1175/1520-0477(1996)077<0437:TNYRP>2.0.CO;2

Marshall, L. R., Maters, E. C., Schmidt, A., Timmreck, C., Robock, A., & Toohey, M. (2022). Volcanic effects on climate: Recent advances and future avenues. *Bulletin of Volcanology*, *84*(5), 1–14. https://doi.org/10.1007/s00445-022-01559-3

Mastin, L. G. (2007). A user-friendly one-dimensional model for wet volcanic plumes. *Geochemistry, Geophysics, Geosystems*, *8*(3). https://doi.org/10.1029/2006GC001455

Mastin, L. G. (2014). Testing the accuracy of a 1-D volcanic plume model in estimating mass eruption rate. *Journal of Geophysical Research: Atmospheres*, *119*(5), 2474–2495. https://doi.org/10.1002/2013JD020604

Mastrandrea, M. D., Field, C. B., Stocker, T. F., Edenhofer, O., Ebi, K. L., Frame, D. J., et al. (2010). Guidance note for lead authors of the IPCC fifth assessment report on consistent treatment of uncertainties. Retrieved from https://www.ipcc.ch/site/assets/uploads/2017/08/AR5_Uncertainty_Guidance_Note.pdf

McCormick, M. P., Thomason, L. W., & Trepte, C. R. (1995). Atmospheric effects of the Mt Pinatubo eruption. *Nature*, *373*(6513), 399–404. https://doi.org/10.1038/373399a0

Mulcahy, J. P., Jones, C. G., Rumbold, S. T., Kuhlbrodt, T., Dittus, A. J., Blockley, E. W., et al. (2023). UKESM1.1: Development and evaluation of an updated configuration of the UK Earth System Model. *Geoscientific Model Development*, *16*(6), 1569–1600. https://doi.org/10.5194/gmd-16-1569-2023

Neely, R. R., III, & Schmidt, A. (2016). VolcanEESM: Global volcanic sulphur dioxide (SO_2) emissions database from 1850 to present - Version 1.0 [Dataset]. Centre for Environmental Data Analysis. https://doi.org/10.5285/76ebdc0b-0eed-4f70-b89e-55e606bcd568

O'Neill, B. C., Tebaldi, C., van Vuuren, D. P., Eyring, V., Friedlingstein, P., Hurtt, G., et al. (2016). The Scenario Model Intercomparison Project (ScenarioMIP) for CMIP6. *Geoscientific Model Development*, *9*(9), 3461–3482. https://doi.org/10.5194/gmd-9-3461-2016

Pausata, F. S. R., Chafik, L., Caballero, R., & Battisti, D. S. (2015). Impacts of high-latitude volcanic eruptions on ENSO and AMOC. *Proceedings of the National Academy of Sciences*, *112*(45), 13784–13788. https://doi.org/10.1073/pnas.1509153112

Santer, B. D., Bonfils, C., Painter, J. F., Zelinka, M. D., Mears, C., Solomon, S., et al. (2014). Volcanic contribution to decadal changes in tropospheric temperature. *Nature Geoscience*, *7*(3), 185–189. https://doi.org/10.1038/ngeo2098

Schmidt, A., Mills, M. J., Ghan, S., Gregory, J. M., Allan, R. P., Andrews, T., et al. (2018). Volcanic radiative forcing from 1979 to 2015. *Journal of Geophysical Research: Atmospheres*, *123*(22), 12491–12508. https://doi.org/10.1029/2018JD028776

Sigl, M., Toohey, M., McConnell, J. R., Cole-Dai, J., & Severi, M. (2022). Volcanic stratospheric sulfur injections and aerosol optical depth during the Holocene (past 11 500 years) from a bipolar ice-core array. *Earth System Science Data*, *14*(7), 3167–3196. https://doi.org/10.5194/essd-14-3167-2022

Sigl, M., Winstrup, M., McConnell, J. R., Welten, K. C., Plunkett, G., Ludlow, F., et al. (2015). Timing and climate forcing of volcanic eruptions for the past 2,500 years. *Nature*, *523*(7562), 543–549. https://doi.org/10.1038/nature14565

Stoffel, M., Khodri, M., Corona, C., Guillet, S., Poulain, V., Bekki, S., et al. (2015). Estimates of volcanic-induced cooling in the Northern Hemisphere over the past 1,500 years. *Nature Geoscience*, *8*(10), 784–788. https://doi.org/10.1038/ngeo2526

Timmreck, C., Mann, G. W., Aquila, V., Hommel, R., Lee, L. A., Schmidt, A., et al. (2018). The Interactive Stratospheric Aerosol Model Intercomparison Project (ISA-MIP): Motivation and experimental design. *Geoscientific Model Development*, *11*(7), 2581–2608. https://doi.org/10.5194/gmd-11-2581-2018

Zambri, B., Robock, A., Mills, M. J., & Schmidt, A. (2019). Modeling the 1783–1784 Laki eruption in Iceland: 2. Climate impacts. *Journal of Geophysical Research: Atmospheres*, *124*(13), 6770–6790. https://doi.org/10.1029/2018JD029554

References From the Supporting Information

Archibald, A. T., O'Connor, F. M., Abraham, N. L., Archer-Nicholls, S., Chipperfield, M. P., Dalvi, M., et al. (2020). Description and evaluation of the UKCA stratosphere–troposphere chemistry scheme (StratTrop vn 1.0) implemented in UKESM1. *Geoscientific Model Development*, *13*(3), 1223–1266. https://doi.org/10.5194/gmd-13-1223-2020

Aubry, T. J., & Jellinek, A. M. (2018). New insights on entrainment and condensation in volcanic plumes: Constraints from independent observations of explosive eruptions and implications for assessing their impacts. *Earth and Planetary Science Letters*, *490*, 132–142. https://doi.org/10.1016/j.epsl.2018.03.028

Butchart, N. (2014). The Brewer-Dobson circulation. *Reviews of Geophysics*, *52*(2), 157–184. https://doi.org/10.1002/2013RG000448

Clyne, M., Lamarque, J.-F., Mills, M. J., Khodri, M., Ball, W., Bekki, S., et al. (2021). Model physics and chemistry causing intermodel disagreement within the VolMIP-Tambora Interactive Stratospheric Aerosol ensemble. *Atmospheric Chemistry and Physics*, *21*(5), 3317–3343. https://doi.org/10.5194/acp-21-3317-2021

Dhomse, S. S., Emmerson, K. M., Mann, G. W., Bellouin, N., Carslaw, K. S., Chipperfield, M. P., et al. (2014). Aerosol microphysics simulations of the Mt. Pinatubo eruption with the UM-UKCA composition-climate model. *Atmospheric Chemistry and Physics*, *14*(20), 11221–11246. https://doi.org/10.5194/acp-14-11221-2014

Fero, J., Carey, S. N., & Merrill, J. T. (2009). Simulating the dispersal of tephra from the 1991 Pinatubo eruption: Implications for the formation of widespread ash layers. *Journal of Volcanology and Geothermal Research*, *186*(1–2), 120–131. https://doi.org/10.1016/j.jvolgeores.2009.03.011

Gautier, E., Savarino, J., Hoek, J., Erbland, J., Caillon, N., Hattori, S., et al. (2019). 2600-years of stratospheric volcanism through sulfate isotopes. *Nature Communications*, *10*(1), 466. https://doi.org/10.1038/s41467-019-08357-0

Global Volcanism Program. (2022). Volcanoes of the world (v. 4.11.1) [Database]. Distributed by Smithsonian Institution, compiled by Venzke, E. https://doi.org/10.5479/si.GVP.VOTW5-2022.5.0

Guo, S., Bluth, G. J., Rose, W. I., Watson, I. M., & Prata, A. J. (2004). Re-evaluation of SO_2 release of the 15 June 1991 Pinatubo eruption using ultraviolet and infrared satellite sensors. *Geochemistry, Geophysics, Geosystems*, *5*(4). https://doi.org/10.1029/2003GC000654

Hersbach, H., Bell, B., Berrisford, P., Biavati, G., Horányi, A., Muñoz Sabater, J., et al. (2019). ERA5 monthly averaged data on pressure levels from 1979 to present [Dataset]. Copernicus Climate Change Service (C3S) Climate Data Store (CDS). https://doi.org/10.24381/cds.6860a573

Zanchettin, D., Timmreck, C., Khodri, M., Schmidt, A., Toohey, M., Abe, M., et al. (2022). Effects of forcing differences and initial conditions on inter-model agreement in the VolMIP volc-pinatubo-full experiment. *Geoscientific Model Development*, *15*(5), 2265–2292. https://doi.org/10.5194/gmd-15-2265-2022